IEEE Open Journal of Vehicular Technology

Received 23 October 2023; accepted 6 February 2024. Date of publication 13 February 2024;
date of current version 20 March 2024. The review of this article was coordinated by Editor Wen Chen.

Digital Object Identifier 10.1109/OJVT.2024.3365531

Enabling Flexible Arial Backhaul Links for Post Disasters: A Design Using UAV Swarms and Distributed Charging Stations

MOHAMMAD TAGHI DABIRI, MAZEN HASNA (Senior Member, IEEE), NIZAR ZORBA (Senior Member, IEEE), AND TAMER KHATTAB (Senior Member, IEEE)

Department of Electrical Engineering, Qatar University, Doha 2713, Qatar

CORRESPONDING AUTHOR: MAZEN HASNA (e-mail: hasna@qu.edu.qa)

This work was supported in part by the Qatar National Research Fund, QNRF under Grant NPRP13S-0130-200200 and Grant NPRP14C-0909-210008 and in part by the Qatar National Library.

ABSTRACT In this article, our target is to design a permanent long backhaul link using unmanned aerial vehicle (UAV) relays and charge stations (CSs) to transfer data from the nearest core network to disaster area (DA). To this end, we first characterize the communication channel by considering the energy consumption models of the backup UAVs (moving UAVs) and the UAVs in service (hovering UAVs), the position and number of UAVs in service relative to the DA, along with the position of CSs relative to the position of UAVs. Then we define the optimization problem for two different scenarios. First, we design the long backhaul link in such a way that minimizes the implementation cost. In particular, the optimal design includes finding the optimal position for CSs, UAVs in service along with the optimal planning for backup UAVs in such a way as to reduce the implementation cost and guarantee the quality of service of the multi-relay UAV-based wireless backhaul links. The implementation cost is related to the number of CSs, the number of UAVs in service along with the number of backup UAVs. For the second scenario, we assume that the implementation cost is predetermined, and we find the optimal positions for UAVs and CSs along with planning for backup UAVs to minimize the outage probability. By analyzing the effects of optimization parameters, we further propose low complexity sub-optimal algorithms for both scenarios. Then, using simulations, we show that the sub-optimal algorithms achieve a performance that is very close to the optimal solutions.

INDEX TERMS Antenna pattern, backhaul links, charge stations (CSs), positioning, mmWave/THz communication, unmanned aerial vehicles (UAVs).

I. INTRODUCTION

Climate change is supercharging the increasing frequency and intensity of extreme weather that has led to severe storms, flooding, and hurricanes in recent years. Over the recent period of (2016-2022), the United States experienced 122 separate mega disasters that killed at least 5,000 people and cost more than $1 trillion [1]. Also, Europe has seen a sixty percent increase in extreme weather events [2] from the past three decades. Other parts of the world that have never experienced severe weather should be ready and plan for it now, while those who are more used to extreme natural events should be prepared for more [2]. Natural disasters can potentially cut or completely destroy fiber infrastructure in a disaster area (DA). Any disruption to the fragile fiber causes data disconnections that take days to find and repair.

Beside natural disasters, man-made disasters like terrorist attacks, can be more destructive and costly. Terrorist attacks on the telecommunications infrastructure of advanced cities are potentially attractive targets for what might be called "incremental" terrorism [3]. If no physical damage is done to network which is disrupted in an attack, the communications capabilities are likely to be recoverable in a relatively short time [3]. However, terrorist threats can include a simultaneous physical attack on the incoming optical fiber links at unknown and key points in the telecommunication infrastructure, which is time-consuming to find and fix. By carrying

out such attacks, the entire network of the subject area along with applications based on the Internet of Things (IoT) will be unavailable for a long time. Network outage disrupts most of the daily services such as banks, hospitals, transportation, or local government services. It affects the performance of companies and causes heavy financial losses in the stock market. Moreover, the modern power grid relies on the internet to coordinate power plants and without it, power grid would become unbalanced and with outages. In general, developed countries face greater vulnerability to the terrorist attacks on network infrastructure as IoT becomes more widespread in these countries.

In order to prepare against network infrastructure failures due to natural disasters or terrorist attacks, we must look into alternative solutions for fast network recovery until the communication infrastructure is reconnected. Due to the significant progress made in recent years, the use of backhaul satellite links can be offered as an initial solution to quickly connect the urban network to the global network. However, due to the limited capacity, satellite links cannot provide a capacity equivalent to fiber infrastructure, and thus, planning based on satellite links alone is not sufficient. Therefore, in addition to using the capacities of the satellite backhaul solutions, it is necessary to plan for an alternative/additional flexible wireless solutions to connect the network of DA with the nearest core network (CN). In some cases, the distance to the nearest CN may be tens of kilometers and providing an alternative terrestrial wireless backhaul connectivity encounters serious challenges, including creating a line of sight (LoS) between the DA to the nearest CN, especially in forest and mountainous areas [4]. Due to their unique capabilities such as flexibility, maneuverability, and adaptive altitude adjustment, unmanned aerial vehicles (UAVs) can be considered as a promising solution to provide a temporary wireless backhaul connectivity, while improving reliability of backhaul operations [5], [6], [7], [8].

Recently, UAV-based backhaul links have been studied in few works [9], [10], [11], [12], [13], [14], [15], [16], [17], [18], [19], [20], [21], [22], [23]. In [9], the performance of a 3D two-hop UAV-based network is studied for both amplify-and-forward (AF) and decode-and-forward (DF) relaying protocols. A novel wireless architecture is proposed in [10] by reflecting the backhaul signal using aerial-RIS to provide LoS connectivity in an urban area. Both wireless access and backhaul millimeter wave (mmWave) links are analyzed in [11] to address multi path propagation in an urban environment. A dynamic algorithm for integrated access and backhaul systems is proposed in [12] for both UAV positioning and tracking of temporal user/traffic activity. In [13], the authors investigate the successful content delivery performance in the UAV integrated terrestrial cellular networks where each UAV uses mmWave communications for self-backhaul. In [14], the authors studied the security, privacy, intelligence, and energy-efficiency issues faced by swarms of UAVs to address massive connectivity issues to guarantee ultra-high throughput connectivity in extreme or emergency situations. An adaptive deployment scheme is proposed in [15] for a UAV-aided communication network, where the UAV adapts its distance to serve randomly moving users. Age-of-information-based UAV trajectory is studied in [16] for fresh data collection. In [17], [18], the performance of UAV-based mmWave and terahertz (THz) links is investigated when UAVs are equipped with square array antennas. In [19], the authors addressed the joint UAV location and bandwidth allocation problems to maximize the total profit without exceeding the backhaul and access capacities. A novel spectrum management architecture for UAV swarm is proposed in [20] by considering the special feature of mmWave links.

However, the focus of works [9], [10], [11], [12], [13], [14], [15], [16], [17], [18], [19], [20] is to design a short and flexible backhaul/fronthaul link for low-altitude UAVs in urban environments and are not suitable for providing a long backhaul link of several tens of kilometers. Providing a long UAV-based mmWave/THz backhaul link to connect disaster/remote area to the nearest CN was the subject of the recent studies [21], [22], [23]. In [21], the authors design a long fixed-wing UAV-based mmWave backhaul architecture by taking into account the effects of realistic physical parameters. Using multi-rotor UAVs, the performance of a long mmWave link through multiple UAVs is studied in [22], [23] to connect a remote area with the CN taking into account the fluctuation of UAVs. However, UAVs, like many other autonomous vehicular systems, can be very power-hungry and have limited service span. Therefore, without any program to recharge, they cannot be a suitable option for creating reliable backhaul links to connect the DA to the nearest CN for longer times. None of the works [9], [10], [11], [12], [13], [14], [15], [16], [17], [18], [19], [20], [21], [22], [23] has considered the practical problem related to the limited service time of UAVs.

Considering the importance of providing reliable backhaul links for post-disaster network recovery, in this work, we focus on the analysis, design, and feasibility of long UAV-based backhaul links, which consists of a set of UAVs in service, a set of backup UAVs and a set of mobile charge stations (CSs) to provide a permanent long backhaul link. Our goal is to design the considered long backhaul links including the optimal number and position of UAVs in service, and the optimal number and position of CSs along with optimal planning for backup UAVs. To this end, we first characterize the tackled communication channel by considering the energy consumption models of the backup UAVs (moving UAVs) and the UAVs in service (hovering UAVs), along with the channel parameters such as the actual antenna pattern, the intensity of UAVs' instabilities and its effect on antenna misalignment, the position and number of UAVs in service relative to the nearest CN and DA, the position of CSs relative to the position of UAVs, and the effects of large- and small-scale fading channel coefficients. Then, we formulate the optimization problem for two different scenarios. First, we assume that the link length and channel conditions are known and we want to design the backhaul link in such a way that minimizes the implementation cost, while guaranteeing the requested quality of service

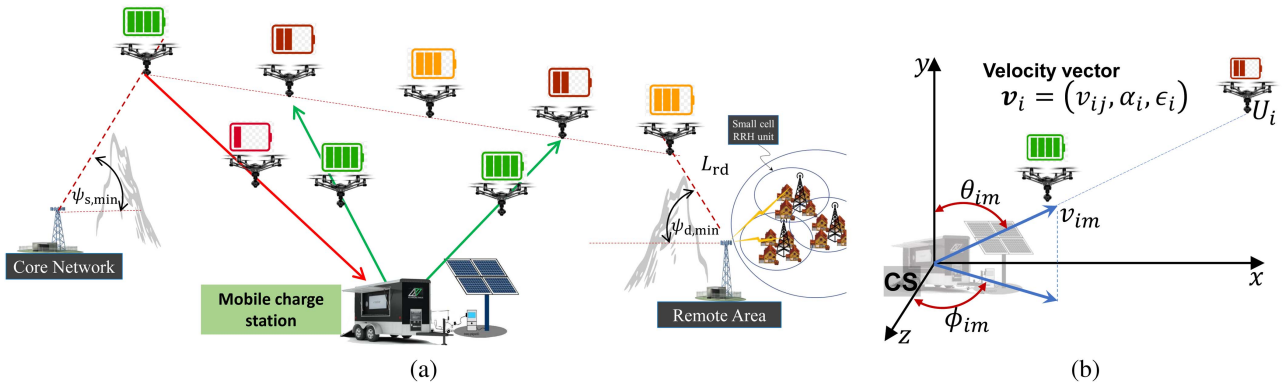

FIGURE 1. (a) An illustration of the considered permanent backhaul links using charge stations and backup UAVs to transfer data from the nearest CN to the DA. (b) The backup UAV flies from C_m toward the U_i with speed vector $\mathbf{v}_i = (v_{im}, \phi_{im}, \theta_{im})$.

(in this work, we target outage probability as the suitable quality of service indicator for such scenario). In the second scenario, for pre-disaster recovery planning, we assume the cost (the number of UAVs and CSs) is known and after the disaster, we try to locate UAVs and CSs along with planning for backup UAVs in such a way to minimize the outage probability. By analyzing the effects of optimization parameters, while simplifying the optimal algorithm, we propose sub-optimal algorithms for both scenarios. Then, using the simulations, we show that the sub-optimal algorithms achieve performance very close to the optimal solutions while their computational load and running time are much less. Moreover, to give a holistic view to the reader, we investigate the effect of key channel parameters as the ratio of the number of UAVs in service to total number of UAVs, the obtained planning for backup UAVs to prevent the UAVs in service from falling, and the number of CSs along with the effect of battery energy density.

II. THE SYSTEM MODEL

We consider a series of UAVs in order to relay data from the nearest CN to the DA as shown in Fig. 1(a) (see Table I for notation). The main challenge of this link is that the UAVs have a limited flight time. Therefore, in order to create a permanent link, it is necessary that along with the UAVs in service, a set of backup UAVs are also available to replace the UAVs in service as shown in Fig. 1(a). Let N_s, N_r, and N_c denote the number of UAVs in service, number of backup UAVs, and number of CSs, respectively, U_i represents the ith UAV in service for $i \in \{1, \ldots, N_s\}$, U_{r_j} is the jth backup UAV for $j \in \{1, \ldots, N_r\}$, and C_m is the mth CS for $m \in \{1, \ldots, N_c\}$. We consider that the nearest CN and DA are at [0, 0, 0] and $[L_{cr}, 0, 0]$ in a Cartesian coordinate system $[x, y, z] \in \mathbb{R}^{1\times 3}$, respectively, where L_{cr} is the link length between CN and DA. Also, $p_{u_i} = (x_{u_i}, y_{u_i}, z_{u_i})$ and $p_{c_m} = (x_{c_m}, y_{c_m}, z_{c_m})$ represent the positions of the ith UAV in service and the mth CS, respectively.

When U_i is running out of charge, to replace it, the backup UAV flies from C_m toward the U_i with speed v_{im}. In particular, the backup UAV flies in a sloping path to reach the U_i where the velocity of the backup UAV in the sloping path is denoted by $\mathbf{v}_i = (v_{im}, \phi_{im}, \theta_{im})$ in spherical coordinate as shown in Fig. 1(b). The parameters ϕ_{im} and θ_{im} are formulated as

$$\begin{cases} \phi_{im} = \tan^{-1}\left((x_{u_i} - x_{c_m})/(z_{u_i} - x_{z_m})\right), \\ \theta_{im} = \tan^{-1}\left(||p_{u_i} - p_{c_m}||/(y_{u_i} - y_{z_m})\right). \end{cases} \tag{1}$$

TABLE 1. List of Main Notations

Parameter	Description
U_i	Denotes ith UAV in service
U_{r_j}	Denotes jth backup UAV
C_m	Denotes mth charge station
N_s	Number of UAVs in service
N_r	Number of backup UAVs
N_c	Number of charge stations
N_{tot}	$N_s + N_r$
$\mathbf{s}_j$	A set of UAVs in service covered by U_{r_j}
M_j	Size of vector $\mathbf{s}_j$ or number of UAVs covered by U_{r_j}
p_{u_i}	$= (x_{u_i}, y_{u_i}, z_{u_i})$ position of U_i
p_{c_m}	$= (x_{c_m}, y_{c_m}, z_{c_m})$ position of C_m
L_{cr}	Link length between CN to DA
L_i	Link length between U_i and U_{i+1} for $i \in \{i, ..., N_s\}$
L_1	Link length between CN and U_1
L_{N_s+1}	Link length between U_{N_s} and DA
L_{im}	Link length between C_m and U_i
v_{im}	speed of backup UAV which flies from C_m to U_i
$\mathbf{v}_i$	$= (v_{im}, \phi_{im}, \theta_{im})$
p_{u_i}	$= (x_{u_i}, y_{u_i}, z_{u_i})$ is the position of U_i
p_{c_m}	$= (x_{c_m}, y_{c_m}, z_{c_m})$ is the position of C_m
$E_{\text{f}_{im}}$	Energy consumption of UAV flying from C_m to U_i
E_{h_i}	Energy consumption of hovering U_i
$\mathbb{P}_{\text{f}_{im}}$	Power consumption of UAV flying from C_m to U_i
$\mathbb{P}_{\text{h}}$	Power consumption of hovering UAV
$t_{f_{im}}$	Flying time from C_m to U_i
t_{h_i}	Hovering time of U_i
t_c	Denote the charging time of each UAV at CS
E_{tot}	Battery capacity of UAV
E_{min}	Minimum UAV energy for flight safety
P_{ou}	End-to-end outage probability of the relay system
$\mathbb{C}\text{ost}$	The cost function defined in (9)

A. UAV POWER CONSUMPTION MODEL

To design the considered system, we need to accurately model the power consumption of the UAV as a function of the flying model and speed. For the considered system, in service mode, UAVs are in hovering mode, and in backup mode, they are in flight mode.

1) FLYING MODE

Following [24], [25], the power consumption of the UAV in the forward flight mode is modeled as follows:

$$\mathbb{P}_{\mathrm{f}_{im}}(v_{im}) = \mathbb{P}_{\mathrm{blade}}(v_{im}) + \mathbb{P}_{\mathrm{fuselage}}(v_{im}) + \mathbb{P}_{\mathrm{induce}}(v_{im}), \quad (2)$$

where $\mathbb{P}_{\mathrm{blade}}(v_{im})$ and $\mathbb{P}_{\mathrm{fuselage}}(v_{im})$ are respectively the required powers to overcome the profile drag forces of the blades, and the fuselage that oppose its forward movement, while, $\mathbb{P}_{\mathrm{induce}}(v_{im})$ is the induced power from the rotation of rotors and they are formulated as [26]:

$$\begin{cases} \mathbb{P}_{\mathrm{blade}}(v_{im}) = M_{\mathrm{rot}}\mathbb{P}_b\left(1+\frac{3v_{im}^2}{v_{\mathrm{tip}}^2}\right), \\ \mathbb{P}_{\mathrm{fuselage}}(v_{im}) = \frac{1}{2}C_D A_f \rho_{\mathrm{cs}} v_{im}^3, \\ \mathbb{P}_{\mathrm{induce}}(v_{im}) = w\cos(\theta_i) + w\sqrt{\left(\sqrt{\frac{w^2}{4M_{\mathrm{rot}}^2\rho_{\mathrm{cs}}^2 A_r^2} + \frac{v_{im}^4}{4}} - \frac{v_{im}^2}{2}\right)}. \end{cases} \quad (3)$$

In (3), $\mathbb{P}_b = \frac{\Delta_p}{8}\rho_{\mathrm{cs}} a A_r v_{\mathrm{tip}}^3$, $\rho_{\mathrm{cs}} = (1 - 2.2558 \times 10^{-5} p_{c_m})^{4.2577}$, v_{tip} is the tip speed of rotors, A_f is the fuselage area, C_d is the drag coefficient, Δ_p is the profile drag coefficient, s is the rotor solidity, M_{rot} is the number of rotors, and w is the weight of UAV in Newton.

2) HOVERING MODE

The UAVs in service are in hovering mode, in which the power consumption of the UAV is modeled as [26]:

$$\mathbb{P}_{\mathrm{h}} = M_{\mathrm{rot}}\mathbb{P}_b + \frac{w^{3/2}}{\sqrt{4M_{\mathrm{rot}}\rho_{\mathrm{cs}}A_r}}. \quad (4)$$

B. CHANNEL MODELING

To relay information by a set of UAVs to the disaster area, we need a point-to-point high-capacity wireless backhaul link. According to the topology, the best option is to use directional high-frequency mmWave or THz links [17]. Let h_i denotes the instantaneous channel coefficients between U_{i-1} to U_i for $i \in \{2, \ldots, N_s\}$, CN to U_1 for $i = 1$, and U_{N_s} to DA for $i = N_s + 1$. The directional UAV-based THz channel can be well modeled as [27]

$$h_i = h_{L_i} h_{a_i} h_{p_i}, \quad (5)$$

where h_{p_i} is the normalized pointing error (or misalignment fading), h_{a_i} is the small-scale fading, G_0 is the maximum antenna pattern gain, $h_{L_i} = h_{Lf} h_{Lm}$ is the channel path loss, $h_{Lf} = (\frac{\lambda}{4\pi L_i})$ is the free-space path loss, $h_{Lm} = e^{-\frac{\mathcal{K}(f)}{2}L_i}$ denotes the molecular absorption loss where $\mathcal{K}(f)$ is the frequency dependent absorption coefficient, and L_i is the link length.

We consider that each U_i has two $N_u \times N_u$ array antennas, one of which is directed to U_{i+1} and the other to U_{i-1}. Directional mmWave/THz links are sensitive to UAV instabilities and cause random misalignment errors known as pointing errors. Following the results of [27, Theorem 1], for a $N_u \times N_u$ array antenna, the distribution of the pointing errors of inter-UAV links is modeled as

$$f_{h_{p_i}}^{\mathrm{u}}(h_{p_i}) = -\frac{\beta_u^2}{G_{u0}^{\beta}} \ln\left(\frac{h_{p_i}}{G_{u0}}\right) \times h_{p_i}^{\beta_u - 1}, \quad (6)$$

where $0 < h_{p_i} < G_{u0}$, $w_{Bu} = \frac{1}{N_u}$ is the antenna beamwidth, $G_{u0} \simeq \pi N_u^2$, $\beta_u = \frac{w_{Bu}^2}{\sigma_u^2}$, and σ_u^2 is the variance of antenna orientation fluctuations of UAV node. Also, following the results of [28, Theorem 2], for a $N_g \times N_g$ array antenna, the distribution of the pointing errors of ground-to-UAV link is modeled as

$$f_{h_{p_i}}^{\mathrm{g}}(h_{p_i}) = \frac{1}{G_{g0}\beta_g - G_{u0}\beta_u}\left[\left(\frac{h_{p_i}}{G_{g0}}\right)^{1/\beta_g - 1} - \left(\frac{h_{p_i}}{G_{u0}}\right)^{1/\beta_u - 1}\right], \quad (7)$$

where $w_{Bg} = \frac{1}{N_g}$ is the antenna beamwidth of the ground station, $\beta_g = \frac{w_{Bg}^2}{\sigma_g^2}$, σ_g^2 is the variance of antenna misalignment of the ground station, and $G_{g0} \simeq \pi N_g^2$.

In THz channels, the α-μ distribution is one of the most widely used models employed for the distribution function of RV h_{a_i} which is given as

$$f_{h_{a_i}}(h_{a_i}) = D h_{a_i}^{\alpha\mu - 1} \exp\left(-W h_{a_i}^{\alpha}\right), \quad (8)$$

where $\alpha > 0$ reflects the nonlinearity of the fading channel, μ is the normalized variance of the fading channel envelope, $D = \frac{\alpha\mu^{\mu}}{\hat{h}_a^{\alpha\mu}\Gamma(\mu)}$, $W = \frac{\mu}{\hat{h}_a^{\alpha}}$, and $\hat{h}_a$ is the α-root mean value of the fading channel envelope.

III. PROBLEM FORMULATION

To design the considered system, we tackle two different optimization approaches that match realistic setups, which are explained below.

A. MINIMIZATION OF THE COST FUNCTION

The cost of implementing such a system includes the number of UAVs in service, the number of backup UAVs, and the number of CSs, which is formulated as:

$$\mathbb{C}\mathrm{ost} = (N_s + N_r)\mathbb{C}\mathrm{ost}_u + N_c\mathbb{C}\mathrm{ost}_c. \quad (9)$$

where $\mathbb{C}\mathrm{ost}_u$ is the cost of the each UAV, $\mathbb{C}\mathrm{ost}_C$ is the cost of each charge station, and $\alpha_c = \mathbb{C}\mathrm{ost}_c/\mathbb{C}\mathrm{ost}_u$. The goal is to design the considered system in such a way that the cost function is minimized while guaranteeing the requested quality of service (QoS). For wireless links, usually outage probability

(OP) (denoted by P_{ou}) is used as the QoS [29]. To this end, we have

$$P_{\text{ou}} < P_{\text{ou,th}}, \tag{10}$$

where $P_{\text{ou,th}}$ is the threshold OP. The tunable parameters for optimization include two categories of discrete and continuous parameters. The tunable discrete parameters include N_s, N_r and N_c. The tunable continuous parameters include the position of the UAVs in service denoted by p_{u_i} for $i \in \{1, \ldots, N_s\}$, the position of the CSs denoted by p_{c_m} for $m \in \{1, \ldots, N_c\}$, and the speed of the backup UAVs which flies from C_m to U_i denoted by v_{im} for $i \in \{1, \ldots, N_s\}$. In addition to these parameters, another important tunable parameter is the planning for backup UAVs to cover UAVs in service. In particular, how many and which UAVs in service can be covered by the jth backup UAV for $j \in \{1, \ldots, N_r\}$, which we will discuss more in the next section. To formulate this assignment planning for the backup UAVs, we define vector $\mathbf{s}_j = [m_1, \ldots, m_{M_j}]$, which is a vector with M_j elements. M_j specifies the number of UAVs in service supported by the jth backup UAV. For example, $\mathbf{s}_3 = [2, 4, 6, 9]$ indicates that $M_3 = 4$ and U_2, U_4, U_6, and U_9 are covered by U_{r_3}. For this assignment, all UAVs in service must be covered, and vectors $\mathbf{s}_j$ and $\mathbf{s}_i$ should be disjoint (their intersections should be empty) for any $i, j \in \{1, \ldots, N_r\}$ and $i \neq j$, which are formulated as:

$$\begin{cases} \mathbf{s}_1 \bigcap \mathbf{s}_2 \bigcap \ldots \bigcap \mathbf{s}_{N_r} = \emptyset, \\ \sum_{j=1}^{N_r} M_j = N_s. \end{cases} \tag{11}$$

Let $E_i(t)$ represent the instantaneous energy of U_i. In order to prevent U_i from falling while in service, its energy must be greater than a threshold $E_{\min}$, which is expressed as $E_i(t) > E_{\min}$. Also, for flight safety, the speed of the UAV cannot exceed a maximum value as $v_{im} < v_{\max}$. Finally, based on the explanations, the optimization problem to reduce the implementation cost is formulated as follows:

$$\min_{\mathbb{S}_{c1}} \quad \mathbb{C}\text{ost} \tag{12a}$$

$$\text{s.t.} \quad P_{\text{ou}} < P_{\text{ou,th}}, \tag{12b}$$

$$\mathbf{s}_1 \bigcap \mathbf{s}_2 \bigcap \ldots \bigcap \mathbf{s}_{N_r} = \emptyset, \tag{12c}$$

$$\sum_{j=1}^{N_r} M_j = N_s, \tag{12d}$$

$$E_i(t) > E_{\min}, \ i \in \{1, \ldots, N_s\}, \tag{12e}$$

$$v_{im} < v_{\max}, \quad i \in \{1, \ldots, N_s\}, \tag{12f}$$

where the set of tunable parameters $\mathbb{S}_{c1}$ is

$$\mathbb{S}_{c1} = \begin{cases} \{N_s, N_r, N_c\}, \\ p_{c_m}, \ \text{for } m \in \{1, \ldots, N_c\}, \\ p_{u_i}, \ \text{for } i \in \{1, \ldots, N_s\}, \\ v_{im}, \ \text{for } i \in \{1, \ldots, N_s\}, \\ \mathbf{s}_j, \ \text{for } j \in \{1, \ldots, N_r\}. \end{cases} \tag{13}$$

B. MINIMIZATION OF THE OUTAGE PROBABILITY

Optimization problem (12) is suitable for reducing the implementation cost of the system. It is better to optimize the system based on (12) for bad environmental conditions. After the implementation of the system, the number of CSs and UAVs is known, and minimizing the cost is no longer an issue. In this case, with every change of channel conditions, we have to update the optimal system parameters while the number of UAVs and CSs is known. Therefore, after the implementation, the goal is to optimize the system parameters to improve the system performance, or in other words, the OP is minimized. Let N_{tot} be the number of UAVs, which is now a constant parameter. In this case, optimization problem (12) is modified as follows:

$$\min_{\mathbb{S}_{c2}} \quad P_{\text{ou}} \tag{14a}$$

$$\text{s.t.} \quad N_s + N_r = N_{\text{tot}}, \tag{14b}$$

$$\text{(12c), (12d), (12e), and, (12f),} \tag{14c}$$

where the set of tunable parameters $\mathbb{S}_{c1}$ is

$$\mathbb{S}_{c1} = \begin{cases} \{N_s, N_r\}, \\ p_{c_m}, \ \text{for } m \in \{1, \ldots, N_c\}, \\ p_{u_i}, \ \text{for } i \in \{1, \ldots, N_s\}, \\ v_{im}, \ \text{for } i \in \{1, \ldots, N_s\}, \\ \mathbf{s}_j, \ \text{for } j \in \{1, \ldots, N_r\}. \end{cases} \tag{15}$$

The difference between the optimization parameters defined in (13) and (15) is that in (15), N_c is a constant value and we also know that $N_s + N_r = N_{\text{tot}}$.

As can be seen, both optimization problems (12) and (14) are mixed integer nonlinear programming problem. Therefore, in the next section, several sub-optimal algorithms are introduced to solve the above two optimization problems.

IV. OPTIMAL SYSTEM DESIGN

Next, we will try to solve the optimization problem by analyzing the parameters of the considered system. To this end, the positioning of UAVs and CSs is investigated first, and then, with the obtained results, we proceed to optimize of the rest of the parameters.

A. UAVS POSITIONING

Regardless of the rest of the system parameters, the OP is only a function of the UAVs in service and their positions. Therefore, in the following, we first obtain the OP as a function of the number and position of UAVs in service.

1) OUTAGE PROBABILITY ANALYSIS

For the considered decode-and-forward multi-relay system, the OP is obtained as

$$\begin{aligned} P_{\text{ou}} &= \text{Prob}\left[\min(h1, \ldots, h_{N_s+1}) > h_{\text{th}}\right] \\ &= 1 - \text{Prob}\left[h_1 > h_{\text{th}}, \ldots, h_{N_s+1} > h_{\text{th}}\right], \end{aligned} \tag{16}$$

where h_{th} is the channel coefficient threshold. Given that h_is are independent, (16) is simplified as

$$P_{\text{ou}} = 1 - \prod_{i=2}^{N_s} \prod_{j=1,N_s+1} \left(1 - P^{\text{g}}_{\text{ou}_j}\right)\left(1 - P^{\text{u}}_{\text{ou}_i}\right), \tag{17}$$

where $P^{\text{g}}_{\text{ou}_j}$ is the outage probability of the first ($j = 1$) and last link ($j = N_s + 1$), while $P^{\text{u}}_{\text{ou}_i}$ is the outage probability of the inter UAV links for $i \in \{2, \ldots, N_s\}$. Using (5), (6), (8) and following the results of [27], $P^{\text{u}}_{\text{ou}_i}$ is obtained as

$$P^{\text{u}}_{\text{ou}_i} = 1 - \sum_{k=0}^{\mu-1} \frac{B_1 h_{\text{th}}}{\alpha} \frac{a\beta_u^2}{\Gamma(k+1)} \Bigg[(B_1 h_{\text{th}})^{B_2} e^{-\left(\frac{(B_1 h_{\text{th}})^{\alpha}}{2}\right)} \mathbb{W}_{B_3,B_4}\left(B_1^{\alpha} h_{\text{th}}^{\alpha}\right) - (B_1 h_{\text{th}})^{B_5} e^{-\left(\frac{(B_1 h_{\text{th}})^{\alpha}}{2}\right)} \mathbb{W}_{B_6,B_7}\left(B_1^{\alpha} h_{\text{th}}^{\alpha}\right) \Bigg], \tag{18}$$

where $\mathbb{W}_{-\frac{\nu}{2},\frac{1-\nu}{2}}(\cdot)$ is the Whittaker function [30], and

$$\begin{cases} B_1 = \frac{\mu^{1/\alpha}}{G_{u0}\hat{h}_a h_{L_i}}, \quad B_2 = \frac{\alpha(k-1)}{2} + \frac{\beta_u}{2} - \frac{1}{2a} - 1, \\ B_3 = \frac{k-1}{2} - \frac{\beta_u}{2\alpha} + \frac{1}{2a\alpha}, \quad B_4 = B_3 + \frac{1}{2}, \\ B_5 = \frac{\alpha(k-1)}{2} + \frac{\beta_u}{2} - 1, \quad B_6 = \frac{k-1}{2} - \frac{\beta_u}{2\alpha}, \\ B_7 = B_6 + \frac{1}{2}. \end{cases}$$

Also, using (5), (7), (8) and following the results of [28], $P^{\text{g}}_{\text{ou}_j}$ is obtained as

$$P^{\text{g}}_{\text{ou}_j} \simeq 1 - \frac{1}{\alpha(\beta_g - \beta_u)} \sum_{k=0}^{\mu-1} \frac{(A_2 \mathbb{A}_0(h_{\text{th}}))^{k-1}}{\Gamma(k+1)} e^{-\frac{A_2 \mathbb{A}_0(h_{\text{th}})}{2}} \times \Bigg[(A_2 \mathbb{A}_0(h_{\text{th}}))^{\frac{V_3}{2}} \mathbb{W}_{\frac{-V_3}{2},\frac{1-V_3}{2}}(A_2 \mathbb{A}_0(h_{\text{th}})) - (A_2 \mathbb{A}_0(h_{\text{th}}))^{\frac{V_4}{2}} \mathbb{W}_{\frac{-V_4}{2},\frac{1-V_4}{2}}(A_2 \mathbb{A}_0(h_{\text{th}})) \Bigg], \tag{19}$$

where

$$\begin{cases} V_1 = (1/\alpha\beta_g - \mu + 1), \quad V_2 = (1/\alpha\beta_u - \mu + 1), \\ V_3 = (1/\alpha\beta_g - k + 1), \quad V_4 = (1/\alpha\beta_u - k + 1), \\ \mathbb{A}_0(h_{\text{th}}) = \left(\frac{h_{\text{th}}}{G_0 h_L}\right)^{\alpha}, \quad \mathbb{A}_1(h_{\text{th}}) = \frac{A_2\alpha^2}{2}\mathbb{A}_0(h_{\text{th}}), \\ \mathbb{A}_2(h_{\text{th}}) = \frac{(A_3 - \mathbb{A}_1(h_{\text{th}})/\alpha)^2}{\mathbb{A}_1(h_{\text{th}})}, \quad A_2 = \frac{\mu}{\hat{h}_a^{\alpha}}, \\ A_1 = \frac{\alpha\mu^{\mu}}{\hat{h}_a^{\alpha\mu}\Gamma(\mu)}, \quad A_3 = \alpha\mu - \frac{1}{\min(\beta_u, \beta_g)}. \end{cases}$$

2) POSITIONING TO MINIMIZE THE COST

The outage probability provided in (17) is a function of all the real channel parameters, such as the number of UAVs in service, positions of the UAVs, antenna pattern, UAVs' vibrations, link length, and small-scale fading. For the optimization problem (12), condition (12b) must be satisfied, which is directly related to the positioning of U_is. Let L_1, L_{N_s+1} represent the link lengths of the first ground-to-UAV (GU) link and last UAV-to-ground (UG) links, respectively, and L_i for $i \in \{2, \ldots, N_s\}$ represent the links between U_{i-1} and U_i. According to the symmetry of the problem, we know that the inter-UAV links are equal, i.e., $L_i = L_j$ for $i \in \{2, \ldots, N_s\}$. Therefore, the optimal solution is simplified to find the three continuous parameters L_1, L_2, L_{N_s+1} and N_s which is formulated as:

$$\min_{L_1, L_2, L_{N_s+1}, N_s} \quad N_s \tag{20a}$$

$$\text{s.t.} \quad P_{\text{ou}} < P_{\text{ou,th}}. \tag{20b}$$

Based on (17), (18), and (19), these parameters L_1, L_2, L_{N_s+1}, and N_s are correlated together. Therefore, optimization problem (20a) is a 4-dimensional optimization problem with three continuous variables and one discrete variable.

As a sub-optimal method, for the low OPs, (17) can be simplified as:

$$P_{\text{ou}} \simeq \sum_{i=2}^{N_s} P^{\text{u}}_{\text{ou}_i} + \sum_{j=1,N_s+1} P^{\text{g}}_{\text{ou}_j}. \tag{21}$$

We also assume that the UAVs are positioned in such a way that the OP between all links is equal. Using this and based on (19), and (21), the parameters L_1 and L_{N_s+1} are obtained separately as:

$$\begin{cases} L_{1,\text{opt}} = \min\limits_{L_1} \left| P^{\text{g}}_{\text{ou}_1}(L_1) - \frac{P_{\text{ou,th}}}{N_s+1} \right|, \\ L_{N_s+1,\text{opt}} = \min\limits_{L_{N_s+1}} \left| P^{\text{g}}_{\text{ou}_{N_s+1}}(L_{N_s+1}) - \frac{P_{\text{ou,th}}}{N_s+1} \right|. \end{cases} \tag{22}$$

Note that the term $|P^{\text{g}}_{\text{ou}_j}(L_j) - \frac{P_{\text{ou}}}{N_s+1}|$ is a Convex function of L_j and as a result, the sub-optimal value for L_1 and L_{N_s+1} are easily obtained from (22). Using obtained L_1 and L_{N_s+1}, the position of U_1 and U_{N_s} are computed as

$$\begin{cases} p_{u_1} = \left(L_1 \cos(\psi_{s,\min})), L_1 \sin(\psi_{d,\min})), 0\right), \\ p_{u_{N_s}} = \left(L_{N_s+1} \cos(\psi_{s,\min})), L_{N_s+1} \sin(\psi_{d,\min})), 0\right), \end{cases} \tag{23}$$

where $\psi_{s,\min}$ and $\psi_{d,\min}$ are respectively the minimum acceptable elevation angles of CN and DA to provide LoS connectivity for considered THz links as shown in Fig. 1(a). Now, using (18) and (21), the maximum acceptable value of L_i for $i \in \{2, \ldots, N_s\}$ is derived as

$$L_{\text{i,max}} = \min_{L_i} \left| P^{\text{u}}_{\text{ou}_i}(L_i) - \frac{P_{\text{ou,th}}}{N_s + 1} \right|. \tag{24}$$

Since the number of UAVs is an integer variable, it is not possible to reach the value obtained in (24) for L_i. However, (24) tells us that the UAVs should be placed on the connecting line between p_{u_1} and $p_{u_{N_s}}$ with equal distances in such a way that the distance between the UAVs is not greater than $L_{\text{i,max}}$. Therefore, the sub-optimal values for L_i and N_s are obtained as:

$$\begin{cases} N_{s,\text{opt}} = \max\limits_{N_s} \frac{L_{1,N_s}}{N_s - 1}, \\ L_{i,\text{opt}} = \frac{L_{1,N_s}}{N_{s,\text{opt}} - 1}, \end{cases} \tag{25}$$

where

$$L_{1,N_s} = \sqrt{(x_{u_1} - x_{u_{N_s}})^2 + (y_{u_1} - y_{u_{N_s}})^2}. \tag{26}$$

Algorithm 1: Sub-optimal UAVs Positioning to Minimize N_s.

Input: Environmental and geometrical channel parameters
Output: N_s, p_{u_i} for $i \in \{1, \ldots, N_s\}$
1: Find L_1, and L_{N_s+1} from (19) and (22).
2: Compute p_{u_1} and $p_{u_{N_s}}$ using (23).
3: Find N_s and L_i for $i \in \{2, \ldots, N_s\}$ using(18), (24), and (25).
4: Compute p_{u_i} for $i \in \{2, \ldots, N_s - 1\}$ using (27) and (28).

Using results of (25), the sub-optimal position of U_i for $i \in \{2, \ldots, N_s - 1\}$ is obtained as:

$$\begin{cases} x_{u_i} = x_{u_1} + (i-1)L_i \cos(\theta_{1N_s}), \\ y_{u_i} = y_{u_1} + (i-1)L_i \sin(\theta_{1N_s}), \end{cases} \tag{27}$$

where

$$\theta_{1N_s} = \tan^{-1}\left(\frac{y_{u_{N_s}} - y_{u_1}}{x_{u_{N_s}} - x_{u_1}}\right). \tag{28}$$

In Algorithm 1, the sub-optimal method is provided to find N_s, and p_{u_i}s, which is much faster than the 4-dimensional optimization problem (20a).

Remark 1: Considering that the value of N_s is discrete, in the simulations, it is shown that in most cases, the sub-optimal value of N_s obtained from Algorithm 1 is equal to the optimal value obtained from (20a).

3) POSITIONING TO MINIMIZE THE OP

In this case, because $N_{\text{tot}} = N_s + N_r$ is known, then the optimal number of N_s depends on N_r. However, for each N_s, the optimal position for U_is is obtained as:

$$\min_{L_1, L_2, L_{N_s+1}} \quad P_{\text{ou}} \tag{29a}$$

$$\text{s.t.} \quad L_1 \cos(\psi_{s,\min}) + L_{N_s+1} \cos(\psi_{d,\min}) + (N_s - 1)L_2 \cos(\theta_{1N_s}) = L_{\text{cr}}. \tag{29b}$$

As a sub-optimal method, we assume that $P^{\text{u}}_{\text{ou}_i} \simeq P^{\text{g}}_{\text{ou}_j}$. Therefore, for each L_2, we can calculate L_1 and L_{N_s+1} as:

$$\begin{cases} L_{1,\text{opt}} \simeq \min\limits_{L_1} \left| P^{\text{g}}_{\text{ou}_1}(L_1) - P^{\text{u}}_{\text{ou}_2}(L_2) \right|, \\ L_{N_s+1,\text{opt}} \simeq \min\limits_{L_{N_s+1}} \left| P^{\text{g}}_{\text{ou}_{N_s+1}}(L_{N_s+1}) - P^{\text{u}}_{\text{ou}_2}(L_2) \right|. \end{cases} \tag{30}$$

Using (30), for any given N_s, Algorithm 2 is provided to find the sub-optimal values of L_is. The parameter L_{pric} in Algorithm 2 is defined for the accuracy of the calculations.

Remark 2: In (30), the parameters L_1 and L_{N_s+1} are convex functions of the terms $\mathbb{J}_1 = |P^{\text{g}}_{\text{ou}_1}(L_1) - P^{\text{u}}_{\text{ou}_2}(L_2)|$ and $\mathbb{J}_{N_s+1} = |P^{\text{g}}_{\text{ou}_{N_s+1}}(L_{N_s+1}) - P^{\text{u}}_{\text{ou}_2}(L_2)|$, respectively. We also know that $L_1 > L_{N_s+1}$. Using this information in lines 2 and 10 of Algorithm 2, it can be seen that the algorithm converges quickly.

Algorithm 2: Positioning of UAVs in Service to Minimize the OP for any Given N_s.

Input: N_s, L_{cr}, $\psi_{s,\min}$, $\psi_{d,\min}$, L_{pric}
Input: $\{L_1, \ldots, L_{N_s+1}\}$
Initialize $L_2 = L_{cr}/(N_s + 1)$.
Initialize $L_{2,max} = L_{cr}/(N_s + 1)$, $L_{2,min} = 0$.
Initialize $P_{ou,min} = 1$.
1: Compute $P^{\text{u}}_{\text{ou}_2}$ from (18).
2: Find L_1 and L_{N_s+1} from (30) using (19).
3: Compute L'_{sd} from (29b).
4: **while** $|L'_{\text{sd}} - L_{\text{cr}}| > L_{\text{pric}}$ **do**
5: **if** $L'_{\text{sd}} < L_{\text{cr}}$ **then**
6: Update $L_{2,\max} = L_2$, and $L_2 = \frac{L_2 + L_{2,\max}}{2}$.
7: **else**
8: Update $L_{2,\min} = L_2$, and $L_2 = \frac{L_2 + L_{2,\min}}{2}$.
9: **end if**
10: **Do** lines 1-3 and update L_1, L_{N_s+1}, and L'_{sd}.
11: **end while**

For the proof of Remark 2, please refer to Appendix A.

Remark 3: It should be noted that, unlike Algorithm 1, in Algorithm 2, we cannot determine N_s because we need to know N_r, while N_r itself is a function of other parameters that will be discussed further.

B. POSITIONING OF CS

The position of charge stations is a function of N_s, N_r, N_c, and the position of UAVs in service. For any given N_s and N_c, we have:

$$\min_{p_{c_m}, N_r} \quad N_r \tag{31a}$$

$$\text{s.t.} \quad x_{c_m} = x'_m + x_{u_1} + (2m-1)\frac{x_{u_{N_s}} - x_{u_1}}{2N_c} \tag{31b}$$

$$\min(0, \text{sign}(\theta_{1N_s})X) \geq x'_m \geq \max(0, \text{sign}(\theta_{1N_s})X), \tag{31c}$$

where the parameter X is a function of θ_{1N_s} used to limit the search interval and increase the optimization time.

Remark 4: To find the optimal position for CSs, as starting points, we fist find the the sub-optimal positions p_{c_m} for $m \in \{1, \ldots, N_c\}$ as

$$p_{c_m} = \left[x_{u_1} + (2m-1)\frac{x_{u_{N_s}} - x_{u_1}}{2N_c}, 0, 0 \right]. \tag{32}$$

Then, according to whether θ_{1N_s} is positive or negative, the optimal positions shift towards the disaster area or CN.

For the proof of Remark 2, please refer to Appendix B. Using the results of Remark 4 helps us to limit the range of optimal positions for CSs and increase the speed of solving the optimal problem.

C. OPTIMAL PLANNING FOR BACKUP UAVS

Having optimal planning for backup UAVs helps to reduce the implementation cost and the replacement time. Designing

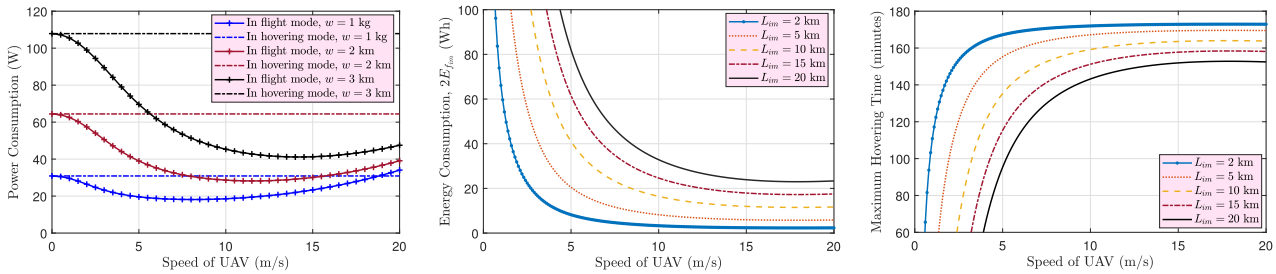

(a) (b) (c)

FIGURE 2. Investigating the effect of UAV's speed on (a) power consumption for different UAV's weight; (b) Energy consumption for different flying lengths; and (c) maximum obtained hovering time for different flying lengths of backup UAV.

an optimal plan for backup UAVs includes finding the optimal vectors $\mathbf{s}_j$ for $j \in \{1, \ldots, N_r\}$ along with the UAVs' speed v_{im}s to manage the time and energy consumption of backup UAVs.

1) SIMPLE SUB-OPTIMAL SOLUTION

As a sub-optimal and simple solution, we backup one UAV for each UAV in service, i.e. $N_s = N_r$. In this case, there is no need to optimize $\mathbf{s}_j$ and v_{im}. In simulations, the performance of this method is compared with the rest of the proposed algorithms.

2) OPTIMAL FLIGHT SPEED

To prevent UAV crashes and based on (12e), for all U_is we must to have:

$$E_{\text{tot}} - 2E_{f_{im}}(\theta_{im}, v_{im}) - E_{h_i} \geq E_{\min}, \tag{33}$$

where E_{tot} is the maximum battery capacity or energy of the UAV, $E_{f_{im}}(\theta_{im}, v_{im}) = \mathbb{P}_{f_{im}}(\theta_{im}, v_{im})t_{f_{im}}$ is the energy consumption of UAV to fly from C_m to U_i with flight time $t_{f_{im}} = \frac{L_{im}}{v_{im}}$, $E_{h_i} = \mathbb{P}_h t_{h_i}$, is the energy consumption of hovering U_i during service time t_{h_i}. Moreover, L_{im} is the link length from C_m to U_i, and θ_{im} is its Zenith angle as shown in Fig. 1(b), which are formulated as:

$$\begin{cases} L_{im} = \sqrt{(x_{u_i} - x_{c_m})^2 + (y_{u_i} - y_{c_m})^2}, \\ \theta_{im} = \tan^{-1}\left(\frac{y_{u_i} - y_{cm}}{|x_{u_i} - x_{cm}|}\right). \end{cases} \tag{34}$$

Optimal flight speed v_{im} is a function of L_{im} and t_{h_i}. For any given L_{im}, the optimal v_{im} is equal to the speed that maximizes the hovering time of U_i. Therefore, we have:

$$\max_{v_{im}} \quad t_{h_i} = \frac{E_{\text{tot}} - E_{\min} - \mathbb{P}_{f_{im}}(\theta_{im}, v_{im})\frac{L_{im}}{v_{im}}}{\mathbb{P}_{\text{h}}} \tag{35a}$$

$$\text{s.t.} \quad v_{im} < v_{\max}. \tag{35b}$$

To get a better view, in Fig. 2(a)–(c), we respectively plot the power consumption, energy consumption, and hovering time versus v_{im}. The result of Fig. 2(a) shows that the optimal selection of v_{im} is important to minimize the power consumption. However, it should be noted that although the power consumption may be reduced by reducing the speed, it increases the flight time and increases the energy consumption. Therefore, in Fig. 2(b) and (c), we have drawn energy consumption and hovering time over a wide range of ($L_{im} = 2 - 20$ km). It can be easily concluded that the optimal value for v_{im} is the maximum acceptable value, i.e., $v_{im} = v_{\max}$, where $v_{\max}$ is the maximum allowed speed of the UAV to ensure the safety of the flight. Moreover, the maximum speed during the replacement of UAVs helps us to make the replacement time faster and a backup UAV can cover a larger number of UAVs. Therefore, the maximum hovering time of U_i as a function of L_{im} is obtained as

$$t_{\text{h,max}_i} = \frac{E_{\text{tot}} - E_{\min} - 2P_{f_{im}}(\theta_{im}, v_{\max})\frac{L_{im}}{v_{\max}}}{\mathbb{P}_{\text{h}}}. \tag{36}$$

3) OPTIMAL PLANNING

In order for the jth backup UAV to be able to cover the set of UAVs in service $\mathbf{s}_j$, we must have:

$$t_{h_i} > 2\sum_{i \in \mathbf{s}_j} t_{f_{im}} + M_j t_c, \tag{37}$$

where t_c is the charging time of the UAV at the charge station. To get a better understanding of (37), a graphical example is provided in Fig. 3, where the first backup UAV using the first charging station wants to cover the set of U_1, U_2, and U_3. In this example, we have $\mathbf{s}_1 = [1, 2, 3]$ and $M_j = 3$. As we can see, when the backup UAV replaces U_1, until the time interval of the next replacement, the backup UAV must fly the routes 1-6 specified in Fig. 3. In addition, it needs to be recharged $M_j = 3$ times along the flight. Therefore, to prevent the U_is from falling for $i \in \{1, 2, 3\}$, we must have:

$$t_{h_i} > 2t_{f_{11}} + 2t_{f_{21}} + 2t_{f_{31}} + 3t_c. \tag{38}$$

Using (36) and (37), to prevent the U_is from falling, the following condition must be met:

$$\sum_{i \in \mathbf{s}_j} L_{im} < \frac{v_{\max}}{2}\left(\min\{t_{\text{h,max}_i} \text{ for } i \in \mathbf{s}_j\} - M_j t_c\right). \tag{39}$$

Using the obtained results, as a sub-optimal design of the considered system, we propose Algorithms 3 and 4 to reduce implementation cost and to decrease end-to-end OP, respectively. In Algorithm 3, $\lfloor x \rfloor$ and $\lceil x \rceil$ are the floor and ceil functions of x, respectively. To run Algorithm 3, we already obtained the sub-optimal values for N_s and p_{u_i}s in

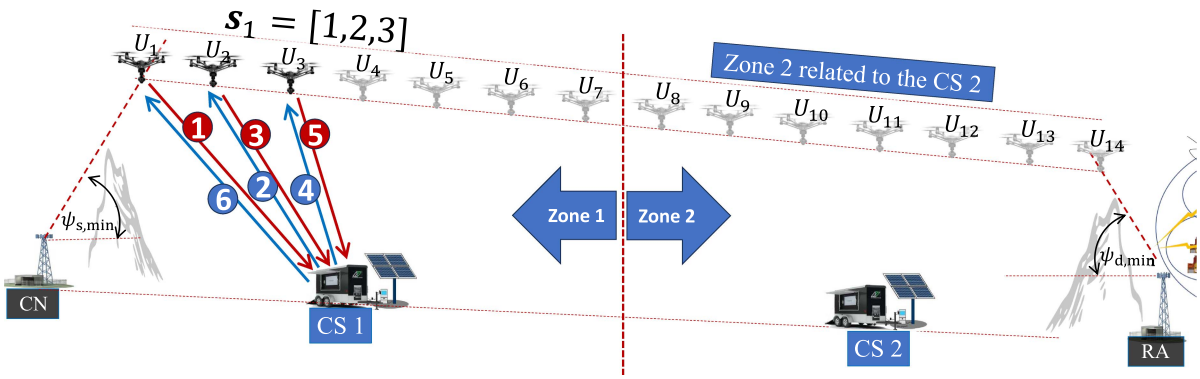

FIGURE 3. Graphical example of planning for the first backup UAV where U_{r1} uses the first CS and covers the set of U_1, U_2, and U_3.

Algorithm 3: Backup Planning to Minimize the Cost for any given N_s.

Input: N_s, p_{u_i}
Output: N_r, N_c, $\mathbb{C}$ost, $\mathbf{s}_j$ for $j \in \{1, \ldots, N_r\}$
Initialize $\mathbb{C}_{ost} = 3N_s$.
1: **for** $N_c = 1 : N_s$ **do**
2: Update $N_r = N_c - 1$.
3: $N_r = N_r + 1, N_r' = N_r, N_s' = N_s, M' = 0$.
4: **for** $j = 1 : N_r$ **do**
5: $M_j = \lfloor N_s'/N_r' \rfloor, m = \lceil jN_c/N_r \rceil$.
6: Compute p_{c_m} using (32).
7: Compute L_{im} using (34) for $i \in 1, \ldots, M_j$.
8: **if** condtion (39) is true for $\sum_{i \in \mathbf{s}_j} L_{im}$ **then**
9: $N_s' = N_s' - M_j, N_r' = N_r' - 1, M' = M' + M_j$.
10: **else**
11: Return to line 3.
12: **end if**
13: **end for**
14: **if** $\mathbb{C}$ost $> N_c + N_r + N_s$ **then**
15: Assign U_is For $i \in \{M' + 1, \ldots, M' + M_j\}$ to $\mathbf{s}_j$.
16: $\mathbb{C}$ost $= N_c + N_r + N_s$.
17: **end if**
18: **end for**

Algorithm 1. Finally, by using Algorithms 1 and 3, a sub-optimal design of the considered system is obtained including the number of UAVs in service and their positions, the number of backup UAVs and their timing and the UAVs covered by them, as well as the number and positions of CSs. Also, by running Algorithm 3, we can reach the optimal design of the considered system, on the condition that we use the optimal values for N_s, and P_{u_i}s obtained in (20), as well as the optimal values for P_{c_m}s obtained in (31). In order to obtain the optimal values in (20) and (31), we use optimization solvers that can reach the solution by exhaustive search. However, to decrease the optimization running time, one can use the obtained sub-optimal results as the initial values and narrow the search range, which increases the optimization speed.

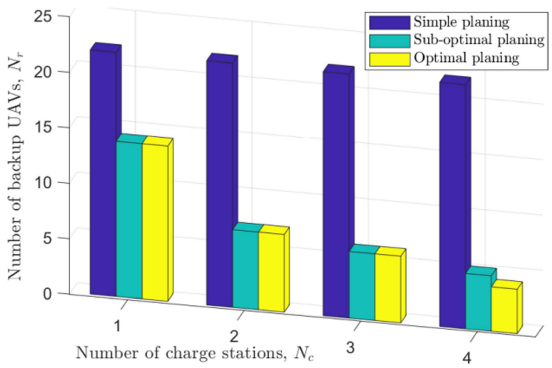

FIGURE 4. Minimum number of obtained backup UAVs from the sub-optimal algorithm versus N_c for a 54 km link length and comparing it with the minimum number of backup UAVs obtained from the optimal and simple planning algorithms.

Algorithm 4: Backup Planning to Minimize the OP when N_c and $N_{\text{tot}} = N_r + N_s$ are known.

Input: N_c, p_{c_m}, N_{tot}
Output: N_s, N_r, P_{ou}
Initialize $N_s = N_{tot}$.
1: Update $N_s = N_s - 1$.
2: Find P_{ou} and p_{u_i} using Algorithm 2.
3: $N_r = N_{\text{tot}} - N_s, N_r' = N_r, N_s' = N_s$.
4: **for** $j = 1 : N_r$ **do**
5: $M_j = \lfloor N_s'/N_r' \rfloor, m = \lceil jN_c/N_r \rceil$.
6: Compute L_{im} using (34) for $i \in 1, \ldots, M_j$.
7: **if** condtion (39) is true for $\sum_{i \in \mathbf{s}_j} L_{im}$ **then**
8: $N_s' = N_s' - M_j, N_r' = N_r' - 1, M' = M' + M_j$.
9: **else**
10: Return to line 1.
11: **end if**
12: **end for**

After designing and implementing the system by Algorithm 3, with every change in channel conditions, we must update the optimal design of the system by Algorithm 4. As we show in the simulations, due to the discreteness

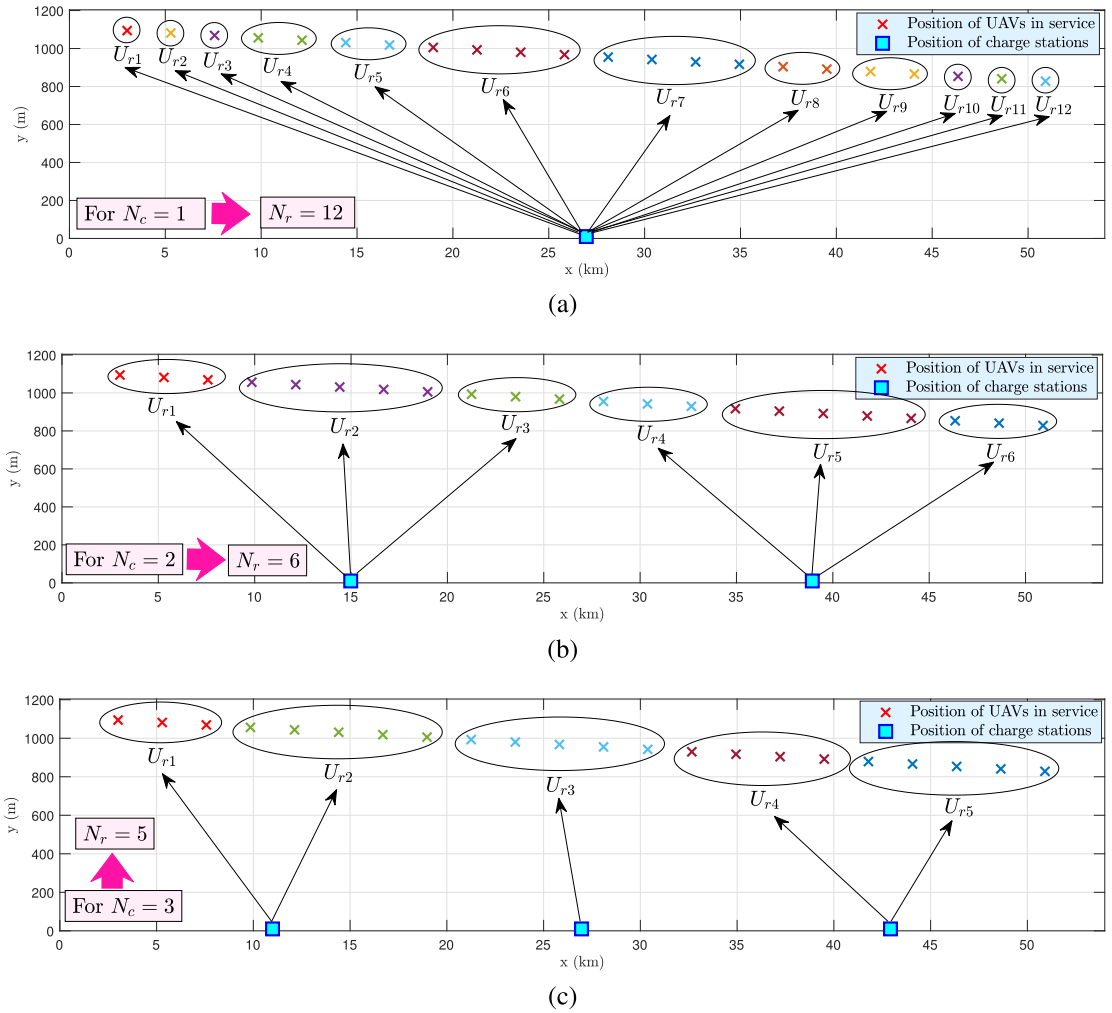

FIGURE 5. Graphical illustration of the results obtained from Fig. 4, including the position of UAVs in service and how they cover by backup UAVs for (a) $N_c = 1$; (b) $N_c = 2$); and (c) $N_c = 3$.

of values of N_s, N_r, and N_c, the results of the sub-optimal algorithms are equal or very close to the optimal values.

V. SIMULATION RESULTS

In this section, using simulations, we evaluate the performance of the considered system. The proposed algorithms were different for the two approaches, in the first step we evaluate the optimal design to reduce the cost of implementation. The parameter values used for simulations are listed in Table 2, which are the commonly used values in the literature [25], [26], [27], [28].

In Fig. 4, for a 54 km link length between the CN and DA, and for a different number of CSs, the minimum number of UAVs required to establish such a link has been obtained using the proposed algorithm. The results of the proposed algorithm are compared with the results obtained from the optimal algorithm. The results of the optimal algorithm have been obtained from an extensive search and the use of MATLAB optimization toolbox according to the explanations provided in the previous section, which is very time-consuming. Also, a simple planning method was provided to assign a backup UAV for each UAV in service. For simulations, the battery capacity of each UAV is considered to be $E_{\text{tot}} = 200$ Wh. From the results of Fig. 4, we understand that the number of UAVs in service to guarantee the requested QoS is equal to 22, because the number of backup UAVs obtained by the

TABLE 2. Parameter Values Used in the Simulation

Parameters	Values	Parameters	Values
w	$10-30$ N	v_{tip}	102 m/s
M_{rot}	6	$v_{\max}$	10 m/s
A_f	0.2 m^2	C_D	0.9
A_r	0.25 m^2	Δ_p	0.0012
$E_{\min}$	10 Wh	E_{tot}	$100-300$ Wh
t_c	20 mins	$P_{\text{ou,th}}$	10^{-2}
σ_{θ_B}	1^o	P_t	7 dBm
L_{cr}	$30-60$ km	N_c	$1-4$
ψ_s	20^o	ψ_d	15^o

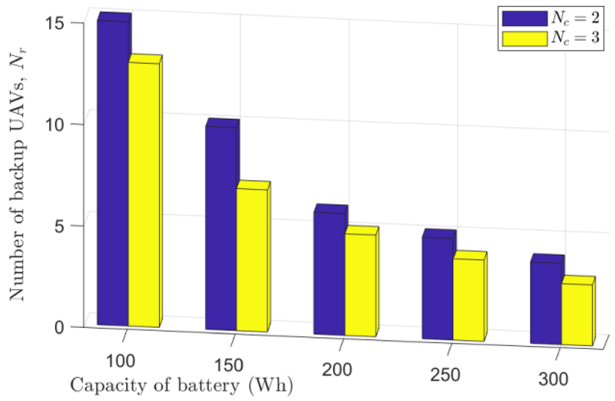

FIGURE 6. Investigating the effect of UAV battery capacity on the number of backup UAVs for two different numbers of N_c.

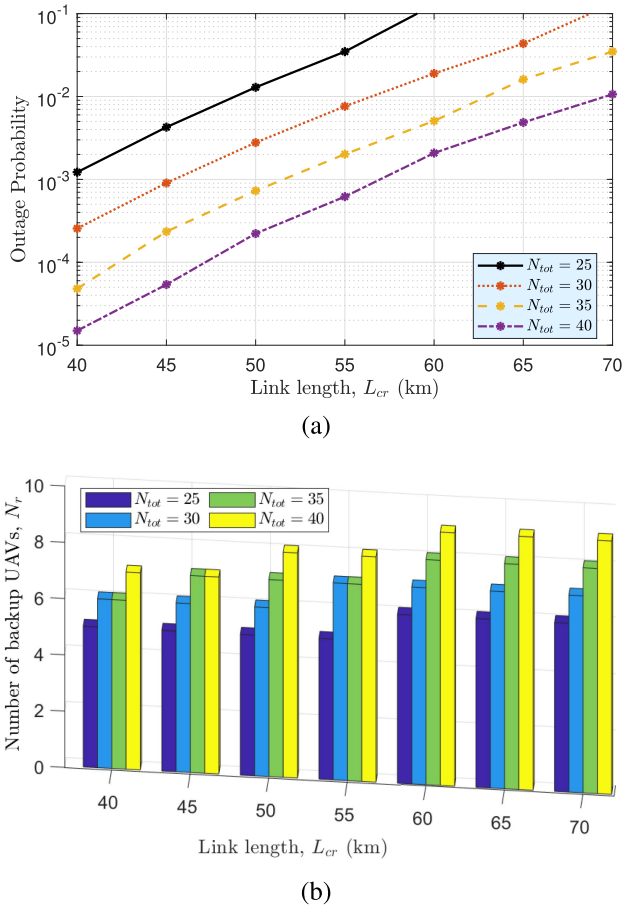

FIGURE 7. (a) Minimum outage probability obtained from Algorithm 4 versus L_{cr} for different values of N_{tot}. (b) Number of backup UAVs obtained from Algorithm 4 versus L_{cr} for different values of N_{tot}.

simple planning method is equal to the number of UAVs in service. As we observe, the proposed sub-optimal algorithm performs much better than the simple planning method, and with a smaller number of backup UAVs, it can guarantee that none of the UAVs in service will crash. Another important point is that the proposed algorithm, despite having lower complexity and computational load, reaches the optimal algorithm performance in most cases. The reason for this is that the variables related to the number of UAVs are discrete.

The results of Fig. 4 only give us information about the minimum number of UAVs and CSs. To get a better view of the results of Fig. 4, the position and clustering of UAVs obtained by the proposed algorithm are shown in Fig. 5(a)–(c). The results show that when only one CS is used, the distance between the CS and the UAVs at the beginning and end of the relay system increases, and as a result, the backup UAV must spend more time and energy to replace the UAVs in service. Therefore, for the number of UAVs with a longer distance, we will have to backup one UAV for each UAV in service. However, by increasing the number of CSs to 2 and 3, we can see that the distance between the CSs and the UAVs in service is reduced and the proposed algorithm can support more UAVs in service with each backup UAV so that UAVs do not fall. However, choosing the optimal number of CSs depends on the cost difference between the CS and the UAV. Usually, in addition to this cost, CSs face the cost of positioning and maintenance, which varies depending on the geographical and environmental conditions.

One of the important parameters affecting the optimal design of the desired system is the battery capacity of the UAV. Unlike surface electrical vehicles, weight is a fundamentally limiting factor in determining the battery capacity of UAVs and makes UAV power systems particularly complex. Today's typical lithium-ion batteries produce around 250 Wh/kg [31]. Lithium Sulfur battery is a next-generation technology, which provides a lighter option for UAV-based applications that require higher energy density [32]. In comparison to the extent lithium-ion battery technologies in the market, lithium Sulfur provides higher energy density (theoretically up to 2600 Wh/kg) [32], [33]. To this end, in Fig. 6, we have analyzed the energy density feature of batteries which is a function of technology and materials. In particular, by considering the same weight for the batteries, we assumed that the batteries have different energy densities and thus, have different capacities. The results of Fig. 6 are obtained for a wide range battery capacity ($E_{\text{tot}} = 100 - 300$ Wh). The results clearly show that by increasing the battery capacity from 100 to 200 Wh, the number of required backup UAVs decreases from 15 to 6. Therefore, choosing the right battery considering the capacity, weight, price, and charging speed is very important in the optimal design of the considered system.

The aim of designing this system is to prepare for critical conditions and quickly establish a backhaul link to the DA from the nearest CN. Therefore, this design should be done before the crisis, and equipment related to UAVs and charging stations should be ready. Therefore, the initial design to reduce the cost of implementation should be done in such a way that covers a wide range of channel link lengths. After the initial design, the number of UAVs N_{tot} and charging stations is known, and we only need to have a positioning and planning

for them using Algorithm 4 to improve the performance of the system. Therefore, in Fig. 7, the performance of Algorithm 4 has been examined for $E_{\text{tot}} = 200$ Wh, $N_c = 2$, and a wide range of link lengths. Based on the results of Fig. 7(a), in order to guarantee the QoS of the backhaul link, $N_{\text{tot}} = 25$ can cover a maximum of 47 km link, while for $N_{\text{tot}} = 30$ and 40, the backhaul link of 57 and 70 km can be covered. Likewise, in Fig. 7(b), using Algorithm 4, the optimal number of backup UAVs according to each link length is provided to achieve the best performance. The results show that with each change in the link length, re-planning is required for the backup UAVs.

VI. CONCLUSION

The main goal of this work is to design a long backhaul link using a set of UAVs to connect the DA to the nearest CN. To this end, we considered two scenarios. In the first scenario, for the case where the physical characteristics of an area (such as the link length, obstacles, wind speed) are known, we proposed an optimal algorithm that, while finding the optimal position for UAVs in service and the optimal position for CSs, it also obtains an optimal planning for backup UAVs so that while guaranteeing the outage probability, the implementation cost decreases. For the second scenario, when the number of UAVs and CSs are known, we proposed an optimal algorithm that finds the optimal positions for UAVs and CSs along with planning for backup UAVs to minimize the outage probability. Finally, by providing simulations, we studied the effect of important parameters such as the number of required UAVs and the number of CSs to provide a reliable long backhaul link. We showed that increasing the number of CSs reduces the flight path in the replacement mode and reduces the number of backup UAVs. Also, the effect of UAV battery capacity and link length on the required number of UAVs was investigated.

APPENDIX A

The function $P^{\text{u}}_{\text{ou}_2}(L_2)$ conditioned on L_2 is constant and positive. Also, $P^{\text{g}}_{\text{ou}_1}(L_1)$ is a positive and ascending function of L_1. Moreover, based on the results of [28], for $L_1 = L_2$, we have $P^{\text{g}}_{\text{ou}_1}(L_1) \leq P^{\text{u}}_{\text{ou}_2}(L_2)$, which results in the optimal value of $L_1 \in [L_2, \infty]$. Therefore, by increasing L_1 from L_2, first, $P^{\text{g}}_{\text{ou}_1}(L_1)$ increases towards $P^{\text{u}}_{\text{ou}_2}(L_2)$, and thus, $\mathbb{J}_1$ tends to zero. Then, with the further increase of L_1, $P^{\text{g}}_{\text{ou}_1}(L_1)$ becomes larger than $P^{\text{u}}_{\text{ou}_2}(L_2)$, and as a result, $\mathbb{J}_1$ increases again and we can conclude that $\mathbb{J}_1$ is convex function of L_1. Similarly, it can be shown that $\mathbb{J}_{N_s+1}$ is also a convex function of L_{N_s+1}. On the other hand, since the transmission power of the ground station is greater than the UAV due to the UAV's power limitations, for $L_1 = L_2 = L_{N_s+1}$, we always have $P^{\text{g}}_{\text{ou}_1}(L_1) \leq P^{\text{g}}_{\text{ou}_{N_s+1}}(L_{N_s+1}) \leq P^{\text{u}}_{\text{ou}_2}(L_2)$, and thus, we conclude that the following relationship exists between the optimal values of L_1, L_2, and L_{N_s+1} as

$$L_1 \geq L_{N_s+1} \geq L_2. \tag{40}$$

As can be seen, (40) is used in lines 2-10 of Algorithm 2 for faster convergence.

APPENDIX B

As a sub-optimal solution, we assume that $\theta_{1N_s} \simeq 0$. Under this assumption, due to the symmetry, the optimal position of the charge stations is obtained as a function of the position of the UAVs in service as follows:

$$p_{c_m} = \left[x_{u_1} + (2m-1)\frac{x_{u_{N_s}} - x_{u_1}}{2N_c}, 0, 0 \right], \tag{41}$$

for $m \in \{1, \ldots, N_c\}$. For $\theta_{1N_s} < 0$, the UAVs' altitudes at the beginning of the line (UAVs close to the CN) increase, and the UAVs' altitudes at the end of the line (UAVs close to the DA) decrease, which increases the link length between C_m and the UAVs close to the CA, and reduces the link length between C_m and the UAVs close to the DA. Therefore, in this case, compared to the initial position obtained in (41), the optimal position p_{c_m} is shifted towards the CN. Similarly, it can be justified that if $\theta_{1N_s} > 0$, the optimal position p_{c_m} shifts towards the DA.

ACKNOWLEDGMENT

The statements made herein are solely the responsibility of the authors.

REFERENCES

[1] A. B. Smith, "2022 U.S. billion-dollar weather and climate disasters in historical context." Jan. 2023. [Online]. Available: http://www.climate.gov
[2] "5G riders on the storm," [Online]. Available: https://www.teoco.com
[3] N. Council et al. *Information Technology for Counterterrorism: Immediate Actions and Future Possibilities*. Washington, DC, USA: Nat. Academies Press, 2003. [Online]. Available: https://books.google.com.qa/books?id=zQM2eoaWrvEC
[4] B. Galkin, J. Kibilda, and L. A. DaSilva, "Backhaul for low-altitude UAVs in urban environments," in *Proc. IEEE Int. Conf. Commun.*, 2018, pp. 1–6.
[5] M. Alzenad, M. Z. Shakir, H. Yanikomeroglu, and M.-S. Alouini, "FSO-based vertical backhaul/fronthaul framework for 5G+ wireless networks," *IEEE Commun. Mag.*, vol. 56, no. 1, pp. 218–224, Jan. 2018.
[6] W. Khawaja, I. Guvenc, D. W. Matolak, U.-C. Fiebig, and N. Schneckenberger, "A survey of air-to-ground propagation channel modeling for unmanned aerial vehicles," *IEEE Commun. Surveys Tuts.*, vol. 21, no. 3, pp. 2361–2391, thirdquarter 2019.
[7] Q. Wu and R. Zhang, "Common throughput maximization in UAV-enabled OFDMA systems with delay consideration," *IEEE Trans. Commun.*, vol. 66, no. 12, pp. 6614–6627, Dec. 2018.
[8] M. Cui, G. Zhang, Q. Wu, and D. W. K. Ng, "Robust trajectory and transmit power design for secure UAV communications," *IEEE Trans. Veh. Technol.*, vol. 67, no. 9, pp. 9042–9046, Sep. 2018.
[9] M. Banagar and H. S. Dhillon, "3D two-hop cellular networks with wireless backhauled UAVs: Modeling and fundamentals," *IEEE Trans. Wireless Commun.*, vol. 21, no. 8, pp. 6417–6433, Aug. 2022.
[10] H.-B. Jeon, S.-H. Park, J. Park, K. Huang, and C.-B. Chae, "An energy-efficient aerial backhaul system with reconfigurable intelligent surface," *IEEE Trans. Wireless Commun.*, vol. 21, no. 8, pp. 6478–6494, Aug. 2022.
[11] M. Gapeyenko, V. Petrov, D. Moltchanov, S. Andreev, N. Himayat, and Y. Koucheryavy, "Flexible and reliable UAV-assisted backhaul operation in 5G mmWave cellular networks," *IEEE J. Sel. Areas Commun.*, vol. 36, no. 11, pp. 2486–2496, Nov. 2018.
[12] N. Tafintsev et al., "Aerial access and backhaul in mmWave B5G systems: Performance dynamics and optimization," *IEEE Commun. Mag.*, vol. 58, no. 2, pp. 93–99, Feb. 2020.
[13] W. Wang, N. Cheng, Y. Liu, H. Zhou, X. Lin, and X. Shen, "Content delivery analysis in cellular networks with aerial caching and mmWave backhaul," *IEEE Trans. Veh. Technol.*, vol. 70, no. 5, pp. 4809–4822, May 2021.

[14] M. A. Khan et al., "Swarm of UAVs for network management in 6G: A technical review," *IEEE Trans. Netw. Serv. Manage.*, vol. 20, no. 1, pp. 741–761, Mar. 2023.
[15] Z. Wang, L. Duan, and R. Zhang, "Adaptive deployment for UAV-aided communication networks," *IEEE Trans. Wireless Commun.*, vol. 18, no. 9, pp. 4531–4543, Sep. 2019.
[16] C. Zhou et al., "Deep RL-based trajectory planning for AoI minimization in UAV-assisted IoT," in *Proc. 11th Int. Conf. Wireless Commun. Signal Process.*, 2019, pp. 1–6.
[17] M. T. Dabiri, H. Safi, S. Parsaeefard, and W. Saad, "Analytical channel models for millimeter wave UAV networks under hovering fluctuations," *IEEE Trans. Wireless Commun.*, vol. 19, no. 4, pp. 2868–2883, Apr. 2020.
[18] M. T. Dabiri, M. Rezaee, V. Yazdanian, B. Maham, W. Saad, and C. S. Hong, "3D channel characterization and performance analysis of UAV-assisted millimeter wave links," *IEEE Trans. Wireless Commun.*, vol. 20, no. 1, pp. 110–125, Jan. 2021.
[19] C. T. Cicek, H. Gultekin, B. Tavli, and H. Yanikomeroglu, "Backhaul-aware optimization of UAV base station location and bandwidth allocation for profit maximization," *IEEE Access*, vol. 8, pp. 154573–154588, 2020.
[20] Z. Feng, L. Ji, Q. Zhang, and W. Li, "Spectrum management for mmwave enabled UAV swarm networks: Challenges and opportunities," *IEEE Commun. Mag.*, vol. 57, no. 1, pp. 146–153, Jan. 2019.
[21] M. T. Dabiri, M. Hasna, N. Zorba, T. Khattab, and K. A. Qaraqe, "Enabling long mmWave aerial backhaul links via fixed-wing UAVs: Performance and design," *IEEE Trans. Commun.*, vol. 71, no. 10, pp. 6146–6161, Oct. 2023.
[22] M. T. Dabiri, M. O. Hasna, T. Khattab, and K. Qaraqe, "A study of multihop mmW aerial backhaul links," in *Proc. IEEE Int. Wireless Commun. Mobile Comput.*, 2022, pp. 1228–1233.
[23] A. Almohamad, M. T. Dabiri, M. O. Hasna, T. Khattab, and K. Qaraqe, "Long-haul mmWave sky links: A multi-hop NFP-based design and analysis," *IEEE Open J. Veh. Technol.*, vol. 4, pp. 363–374, 2023.
[24] A. Filippone, *Flight Performance of Fixed and Rotary Wing Aircraft*. Amsterdam, The Netherlands: Elsevier, 2006.
[25] N. Babu, M. Virgili, C. B. Papadias, P. Popovski, and A. J. Forsyth, "Cost-and energy-efficient aerial communication networks with interleaved hovering and flying," *IEEE Trans. Veh. Technol.*, vol. 70, no. 9, pp. 9077–9087, Sep. 2021.
[26] N. Babu, I. Donevski, A. Valcarce, P. Popovski, J. J. Nielsen, and C. B. Papadias, "Fairness-based energy-efficient 3-D path planning of a portable access point: A deep reinforcement learning approach," *IEEE Open J. Commun. Soc.*, vol. 3, pp. 1487–1500, 2022.
[27] M. T. Dabiri and M. Hasna, "Pointing error modeling of mmWave to THz high-directional antenna arrays," *IEEE Wireless Commun. Lett.*, vol. 11, no. 11, pp. 2435–2439, 2022.
[28] M. T. Dabiri, M. Hasna, N. Zorba, T. Khattab, and K. A. Qaraqe, "A general model for pointing error of high frequency directional antennas," *IEEE Open J. Commun. Soc.*, vol. 3, pp. 1978–1990, 2022.
[29] R. Imran, M. Odeh, N. Zorba, and C. Verikoukis, "Quality of experience for spatial cognitive systems within multiple antenna scenarios," *IEEE Trans. Wireless Commun.*, vol. 12, no. 8, pp. 4153–4161, Aug. 2013.
[30] I. S. Gradshteyn and I. M. Ryzhik, *Table of Integrals, Series, and Products*. 7th ed. Cambridge, MA, USA: Academic press, 2007.
[31] A. Fotouhi, D. J. Auger, K. Propp, S. Longo, and M. Wild, "A review on electric vehicle battery modelling: From Lithium-ion toward Lithium–Sulphur," *Renewable Sustain. Energy Rev.*, vol. 56, pp. 1008–1021, 2016.
[32] N. Shateri, D. J. Auger, A. Fotouhi, and J. Brighton, "Charging characterization of a high-capacity lithium-sulfur pouch cell for state estimation: An experimental approach," *Energy Storage*, vol. 5, no. 3, 2023, Art. no. e412.
[33] H. Yuan, H.-J. Peng, J.-Q. Huang, and Q. Zhang, "Sulfur redox reactions at working interfaces in lithium–sulfur batteries: A perspective," *Adv. Mater. Interfaces*, vol. 6, no. 4, 2019, Art. no. 1802046.